SEMARAK ILMU PUBLISHING

Journal of Advanced Research in Numerical Heat Transfer

Journal homepage:
https://semarakilmu.com.my/journals/index.php/arnht/index
ISSN: 2735-0142

Finite Element Analysis for Transient on Highly Thermal Hybridization Conductive Ink

Lailatul Hamidah Hamdan[1,2], Mohd Azli Salim[2,*], Nor Azmmi Masripan[2], Chonlatee Photong[3], Alan Watson[4]

[1] Department of Mechanical Engineering, Politeknik Kuching Sarawak (PKS), KM 22, Jalan Matang, Petra Jaya, 93050 Kuching, Sarawak, Malaysia
[2] Fakulti Teknologi dan Kejuruteraan Mekanikal, Universiti Teknikal Malaysia Melaka (UTEM), 75450 Ayer Keroh, Melaka, Malaysia
[3] Faculty of Engineering, Mahasarakham University, Thailand
[4] Power Electronics and Machines Centre, The University of Nottingham, UK

ARTICLE INFO

Article history:
Received 20 January 2025
Received in revised form 23 February 2025
Accepted 25 March 2025
Available online 30 April 2025

Keywords:
Conductive ink; thermal conductivity; substrate; finite element analysis

ABSTRACT

Conductive ink, which can be produced using materials like graphene, possesses exceptional electrical conductivity and is cost-effective as well as environmentally friendly, making it ideal for future printed electronics. The conductive ink's properties also offer significant mechanical strength, excellent heat and electrical conductivity, thermal conductivity, thinness, and flexibility. The hybrid conductive ink, when combined with silver, often demonstrates superior conductivity and stability. This research aims to develop a highly thermal graphene hybrid conductive ink, using graphene nanoparticles, silver flakes, and silver acetate as conductive fillers mixed with chemical and organic solvents. However, reliable data on the finite element analysis (FEA) performance of these mixtures is still lacking. Therefore, to address this, the current study employs an FEA model to simulate total heat flux across various conductive ink perimeters, focusing on substrate size. The models were created using CAD software and analysed in ANSYS Mechanical software to simulate temperature and heat flux. The behaviour of five models with different substrate perimeters was examined using eight thermal conductivity. Additionally, temperature flow and heat flux flow transformation were measured in each model to assess the performance of the hybrid conductive ink. The results show that a 4x4 mm substrate size, with die-attach and diode sizes of 2x2 mm, provides the best performance at the highest thermal conductivity value (350 W/m.K), achieving a total heat flux of up to 6.6 MW/m². Overall, this research illustrates the importance of optimizing substrate size to improve thermal management in hybrid conductive inks.

1. Introduction

Conductive inks, formulated from electrically conductive materials, enable the free movement of electrons when connected to a power source. This is because of their high conductivity, flexibility, affordability, and compatibility with various substrates, conductive inks are essential in printed electronics [1-4]. Typically, based on Camargo *et al.,* [2], conductive ink formulations consist of three

* *Corresponding author.*
E-mail address: azli@utem.edu.my (Mohd Azli Salim)

https://doi.org/10.37934/arnht.35.1.124

primary ingredients: a conductive substance, a binder agent that effectively combines the conductive particles and a solvent that functions to suspend the other ingredients and impart the desired viscosity to the ink based on the printing method chosen. Printed electronics commonly utilize polymer films, paper, and textiles as substrates. Optimizing performance in 2D and 3D electronic devices requires careful selection of printing methods, conductive materials, and substrates to achieve desirable properties such as conductivity, flexibility, and thermal stability [4].

Among conductive materials, graphene is distinguished by its exceptional electrical and thermal properties, such as superior mechanical strength, flexibility, and high thermal conductivity. These attributes make graphene an ideal candidate for next-generation electronic applications [5,6]. Thermal conductivity, measured in watts per meter-kelvin (W/(m·K)), is crucial for optimizing heat transfer efficiency. Enhancing the thermal conductivity of a material can lead to significant cost savings in heat exchanger systems. Researchers, such as Yarmand *et al.,* [7] have investigated the use of suspended solid particles to improve the thermal conductivity of base fluids. Meanwhile, Khanafer *et al.,*[8] and Shekar & Kishan [9] emphasized the need for advanced heat transfer fluids with superior thermal properties. Additionally, the main findings from Sudhindra *et al.,* [10] mentioned that the principal results show that the thermal conductivity of graphene and few-layer graphene can exceed 5000 W/mK, which is exceptionally high. Thermal interface materials (TIMs) based on polymers can significantly increase their thermal conductivity by utilizing this feature. Furthermore, the thermal conductivity of TIMs can be increased up to 25 times above the original polymer by adding graphene or FLG fillers to polymer matrices. Variables including filler concentration, thickness, and lateral dimensions influence the overall thermal performance of graphene/FLG TIMs; bigger lateral dimensions often translate into better thermal conductivity.

Computational modelling, particularly through Finite Element Analysis (FEA), has gained significant attention for solving complex engineering problems [11-13]. Tao [14] proposed methods to improve computational efficiency using ANSYS, addressing challenges such as large deformations, multi-physics phenomena, and thermal-mechanical coupling. Numerous engineering sectors use the FEA widely applied across industries, including automotive, aerospace, and electronics, for analysing heat transfer, dynamics, and structural stability [15-20]. FEA is also used to derive solutions for several classical static structural problems [21]. Outstanding its capacity to predict performance, evaluate the applicability of current features and facilities, optimize new designs, and suggest improvements, FEA is a dependable method of selection.

In the transient thermal simulation, automation and customization are the requirements for the efficiency of the finite element method. Recently, there has been growing interest in modelling the thermal conductivity of hybrid graphene nanoplatelets, silver, and other materials (GNP/Ag) to assess their impact on heat conduction in FEA models [7,12,13]. Additionally, Azli *et al.,* [11] evaluate the stretchability of different ink patterns when subjected to longitudinal and lateral loading using FEA. Despite these advancements, there is limited research on the transient thermal behaviour of hybrid conductive inks, especially concerning the impact of varying substrate sizes and thermal conductivity fluctuations.

This study aims to fill that gap by investigating the effects of different substrate sizes and thermal conductivities on the thermal performance of hybrid conductive inks using FEA. Five models with varying substrate perimeters and eight thermal conductivity values are analysed to assess heat flux and temperature distribution. Based on the superior thermal properties of GNP/Ag hybrids, the hypothesis is that smaller substrates with higher thermal conductivity will demonstrate enhanced heat flux and more uniform temperature distribution. This research aims to contribute to the understanding of how substrate size influences the thermal behaviour of hybrid conductive inks, which has practical applications in printed electronics and thermal management systems.

2. Methodology

The approaches used in this study is to assess the GNP/Ag hybrid die-attach materials' thermal behaviour across a range of substrate sizes are described in this section. The main goal of this study was to identify the GNP/Ag hybrid material's thermal conductivity which, when taken into account with various substrate perimeters, would produce the maximum overall heat flow. Five models with varied substrate sizes were subjected to eight different thermal conductivity values, and the thermal performance of each model was simulated and calculated using Finite Element Analysis (FEA). The objective was to evaluate the effects of heat conduction, which is influenced by thermal conductivity, on the temperature distribution and heat flow in the FEA models. These FEA simulations were carried out using ANSYS Mechanical, which has a track record of accurately predicting performance, assessing design features, optimizing novel configurations, and suggesting possible enhancements. The focus of this study is on heat transmission and thermal conductivity analysis, which makes FEA a suitable method due to its reliability. The material characteristics data, specifically for the GNP/Ag hybrids, were obtained from previous research and pre-existing FEA models, which included temperature and total heat flow calculations. Furthermore, taking particular reference to the work of Kamal *et al.,* [13], this study expands upon earlier studies on graphene-based materials.

2.1 Experiment

The experimental procedure comprised multiple crucial phases to comprehensively assess the characteristics and performance of the GNP/Ag hybrid conductive ink. In order to guarantee a uniform distribution of graphene nanoplatelets and silver particles, the process started with the characterisation of the powder and continued with the mixing step. Following mixing and sintering to improve the link between the particles, the material's mechanical and physical characteristics were examined to determine its strength and structural integrity. Scanning electron microscopy (SEM) was used to investigate the microstructure in order to view the internal structure and guarantee that the conductive particles were bonded and distributed optimally. The GNP/Ag hybrid ink's capacity for heat transfer was then evaluated by measuring its thermal conductivity. Lastly, the information gathered from the mechanical, thermal, and physical testing to perform a Finite Element Analysis (FEA) using ANSYS. This simulation modelled the heat flux and temperature distribution across various substrate sizes, providing insights into the thermal performance of the hybrid conductive ink.

2.1.1 Powder characterization

In order to produce conductive ink, the study focuses on the formulation of GNP hybrid with organic solvents or capping agents as in Figure 1 Process of Cognitive Ink. Finding the ideal mix of organic solvent to combine with a formulation containing silver flake (Ag), silver acetate (SA), and graphene nanoplatelets (GNP), to make a conductive paste is a crucial component of the study. A digital analytical balance was used to properly measure and weigh 0.05 g of precisely measured 25 µm-diameter graphene for the experiment. After being gently set down on the weighing plate, the beaker was given time to stabilize. The beaker's weight was reset using the button on the equipment which functioned until the display read 0.0000 g in order to assure accuracy. Next, fifty millilitres of ethanol were added and covered with aluminium foil. Furthermore, the graphene-ethanol mixture was subjected to sonication for 10 minutes to promote proper dispersion of the GNP within the solvent. In summary, this process is critical for ensuring homogeneity in the paste formulation, which will ultimately affect the performance of the conductive ink.

The use of GNP, Ag and SA in conductive inks improves both thermal conductivity and overall performance. The GNP has high electrical and thermal conductivity helps to improve the ink's heat dissipation capabilities. Its large surface area and good electron mobility enable effective heat transmission, which is critical in applications needing thermal control. In contrast, Ag contribute to the ink's overall stability and conductivity. Their bigger size and high surface-area-to-volume ratio create conductive channels, ensuring that the ink's electrical performance remains consistent. Furthermore, Ag is chemically stable, preventing oxidation and degradation over time, resulting in long-term conductivity. Incorporating SA helps to build conductive Ag networks.

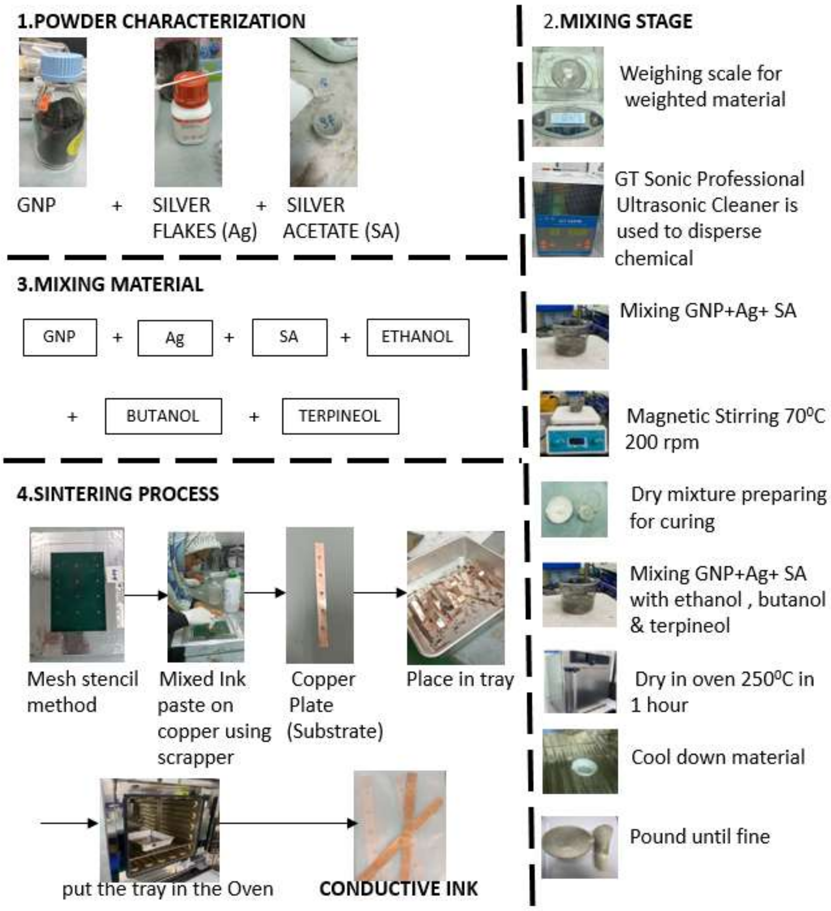

Fig. 1. Process of conductive ink

2.1.2 Mixing stage

After weighing the silver flake, silver acetate, and graphene nanoplatelets, then the mixed silver flake in the ultrasonic bath was stirred for around 1 hour. The same process was also repeated with silver acetate. After finishing the stir of silver flakes, the stirred mixture was dried at 70°C, 200 rpm. Oven-heated at 250°C for an hour, air-dried, cooled. Furthermore, the powder ground was mixed with mortar. Lastly, the mixture was dried, heated, cooled, and ground. Prior to commencing the printing process, the ink pastes creation procedure, which encompasses the formulation for GNP/Ag/SA has been successfully executed. Once the powder has been finely ground, it is accurately weighed to ensure compatibility with the mixture of butanol and terpineol solvents. By using a dropper, the appropriate formulation will be achieved by adding 26 drops of both butanol and terpineol.

The procedure was repeated by employing a Thinky mixer by using the preset coordination. Additionally, this research used Magnetic Stirrer Model SH-3ABE, voltage 220 and heating power is 500W. In this study, the binder and hardener are added to the ink formulation together with a conductive substance, such as graphene, to enable the ink to conduct electricity. After completing GNP/Ag/SA formulation, ink paste is printed on a copper sheet via the mesh stencil method. The procedure begins with applying mixed paste on the grid using a scraper.

2.1.3 Sintering process

The next step in the method is to cure the paste on the substrate for 30 minutes at 250°C in an oven. Particle shape is included in sample characterization for microstructure analysis. Surface microstructure of printed samples evaluated for ink homogeneity using an image analyser. Additionally, the resistivity values of the samples were determined using a multimeter and followed with employing mathematical equations. At last, understanding the conductivity of the samples is of utmost importance in the process.

2.1.4 Physical and mechanical properties evaluation

The mechanical characterization of cognitive ink aimed at obtaining the complete behaviour of different types of substrate size and heat flow, thus, achieving an overview of relevant engineering properties, namely density, porosity, shear strength, shrinkage, and microstructure. The apparatus involved in identifying the classification are optical microscopy, Scanning Electron Microscopy (SEM), and die shear test.

2.1.5 Thermal Conductivity

Thermal conductivity (k) is the capacity of the body to conduct or transmit heat as in Eq. (1) [19].

$$k = \frac{QL}{A\Delta T} \tag{1}$$

where, k is the thermal conductivity in W/m.K, Q is the amount of heat transfer through the material in W, L is the length in m, A is the area of the body in m^2, and ΔT is the difference in temperature in Kelvin unit.

Figure 2 shows the schematic diagram of heat flows in the model and the thickness of each of the materials.

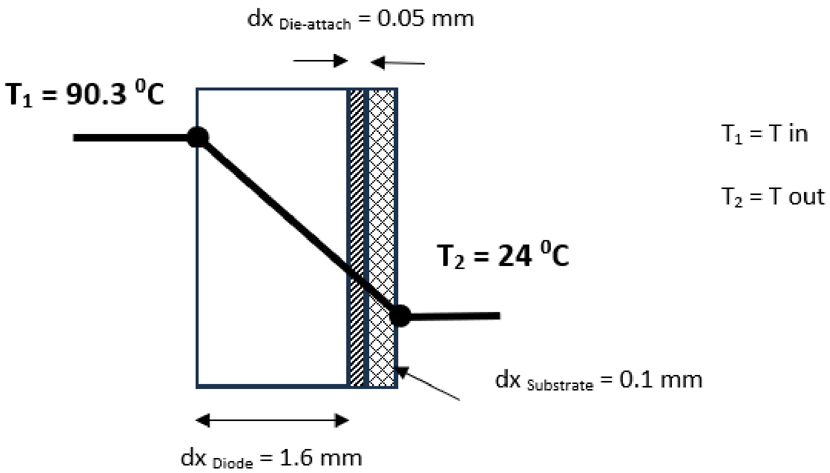

Fig. 2. Schematic diagram of heat flows in the model

2.2 Model Configuration

Finite element modeling (FEM) simulations were performed on a design to predict its performance in terms of temperature and heat flux using ANSYS Mechanical. Because of its capacity to predict performance, evaluate the applicability of current features and facilities, optimize new designs, and suggest improvements, FEA is a dependable method of selection. Data of material properties from prior studies [20,22] and FEA models were used in this study [13,23]. More specifically data from simulations of temperature and total heat flow, as well as previous studies on the properties of graphene materials referring to Kamal *et al.,* [13]. However, the model showed a single-size rectangular design in a 3x3 mm perimeter with diode, die-attach, and substrate width respectively.

The Ansys workbench program, which enables the importation of a geometric layout in CAD format based on model 1 is used to generate the simulation model as an example required in Figure 3. In this research, five types of models have been simulated where the diode and die-attach size have remained 2x2 mm. Despite that, the size of the substrate using copper material increases exponentially from 2x2 mm to 32x32 mm as in Table 1. In one of the models, the substrate perimeter has been identified to be smaller than in Kamal et al., [13] design, to evaluate the effect of small rectangular size. Furthermore, to perceive the performance of the total heat flux, this research has set the various sizes of the substrate which are even larger than the previous researcher. By using the temperature load value on the Mold and the Ansys program, a transient thermal analysis will be carried out in this work to look at temperature and total heat flux changes throughout the graphene conductive ink circuit.

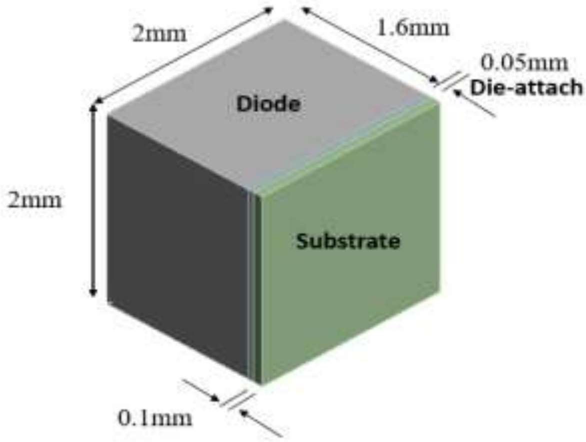

Fig. 3. Isometric view with FEA specifically for Model 1 with perimeter size and thickness

Table 1
Size of each material

Model	Size		
	Diode (SiC)	Die-attach (GNP/Ag)	Substrate (Copper)
1	2x2	2x2	2x2
2	2x2	2x2	4x4
3	2x2	2x2	8x8
4	2x2	2x2	16x16
5	2x2	2x2	32x32

2.3 The Finite Element Analysis

The governing equations are numerically solved at each node using a mesh-generated finite element approach. As shown in Figure 2, the model preference was used in conjunction with the fine mesh choice that can limit the errors without significantly increasing computation time and the Tetrahedrons Patch Confirming (TPC) method. The TPC method creates unstructured tetrahedral mesh in layers based on a specified layer height and fits it to the geometry. Akeremale *et al.,* [18] mentioned the solution in the finite element is independent of the mesh choice. This demonstrates the resilience of the approaches by showing that modifications to the mesh have little to no influence on the temperature distribution. The computation took a while based on the model. When the bigger substrate size is generated, the time to produce is longer, and the space to save also bigger in the computer memory. In the finite element model, this study selected the value 6.5 x 10^{-5} elements size. The relationship between heat flux and material resistance during 1s of heating at temperatures is from 90.3 to 24° C.

Ovrebo [24] mentioned the maximum temperature performed on diodes as semiconductor devices. Meanwhile, the minimum temperature is occupied by the circuit's ambient temperature [13]. The results were achieved by numerically solving the governing equations of fluid dynamics that form the basis for modern computer modelling, known generically as Computational Fluid Dynamics, or CFD. The mesh-generated 3.25 x 10^{-7} finite element approach at each node of 786910 which mesh model of the die-attach sample for 2x2mm substrate perimeter as in Figure 4 and the biggest size is 32x32mm substrate perimeter size as in Figure 5.

Numerous researches have examined the impact of growing substrate size in the contexts of stress measurement and thermal analysis. Qiang *et al.,* [25] address how substrate size influences stress distribution and the uniformity of stress and curvature in deposition processes. Increasing the size results in a stronger nonlinear effect, which may cause surface defects like delamination or cracking. In the meantime, larger substrates have been shown to have an impact on heat flow and thermal conductivity in Mumtaz Rizwee & Deepak Kumar [26]. For example, in material science and additive manufacturing, enlarging the substrate can alter the way heat is transferred and absorbed by the material, which affects the behaviour of thermal stress and strain. Other than that, this perimeter selection is to optimize a proper variety of the printing method, conductive material, ink formulation, and specifically the substrate is critical for achieving optimal printing performance and fabricating 2D and 3D structures and electronic devices with the necessary properties for instance conductivity, optical transparency, thermal stability, flexibility, foldability, resistance to multiple bending [22]. Increasing the size of the substrate in this model is probably an attempt to investigate these impacts on the overall heat flux and thermal distribution in the copper substrate in this research. An observation of variations in total heat flow and thermal behaviour explained the fact that larger substrates have the ability to provide greater heat capacities and distinct temperature gradients throughout the material.

The study uses Finite Element Analysis (FEA) with ANSYS software to do a thorough thermal analysis of conductive inks on a screen-printed circuit. Predicting the circuit's thermal behaviour under varying heating loads requires this analysis, which focuses in particular on how substrate size variation affects thermal conductivity and heat flux distribution. The goal of the study is to investigate the interactions between substrates of various sizes and the various thermal conductivity values seen in hybrid conductive inks. Important variables like as depth, width, thickness, and length will be methodically added to the model to assess how they affect the overall thermal performance. Through an examination of the substrate's impact on temperature dispersion, the research will evaluate how well various designs optimize heat management.

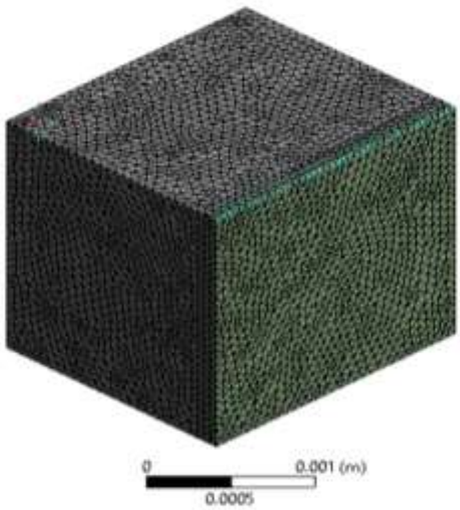

Fig. 4. Mesh model no 1 for 2x2mm substrate size

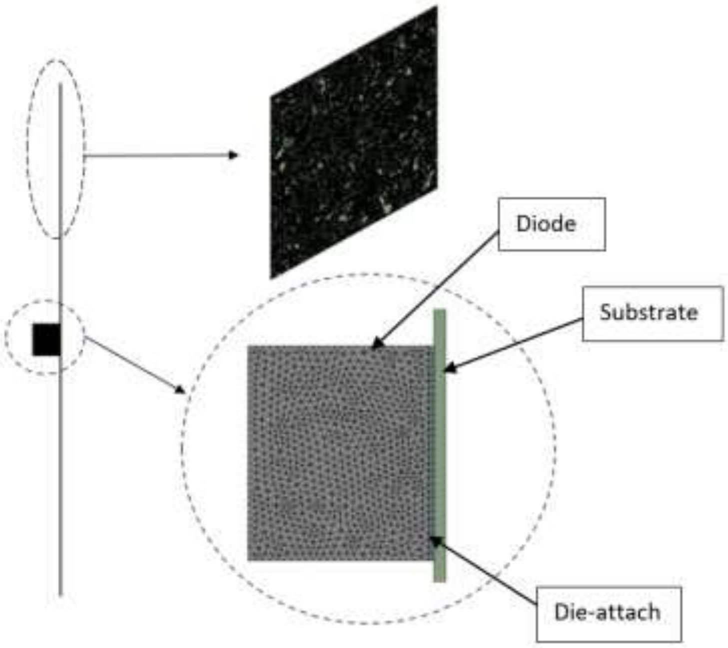

Fig. 5. Mesh model no 5 for 32x32mm substrate size

2.4 Boundary Conditions

The materials that made up the model were identified together with their critical physical characteristics, such as density, specific heat, and thermal conductivity. The devices were silicon (SiC), the circuit substrate was copper, and the bottom of the circuit was die-attach. The highest temperature that was achieved on semiconductor devices, or diodes, was based on [13], which was applied in this investigation. The minimum temperature on SiC die using metallic die-attach materials was 24 °C, while a maximum temperature of 90.3 °C was recorded on the die using epoxy die-attach. The maximum temperature performed on diode as semiconductor devices was referred to Ovrebo [24] and the minimum temperature occupied from the circuit ambient temperature. These results were obtained in the initial attempt to establish simulation baseline findings. Epoxy produced higher temperatures on the SiC diodes than metallic die-attach materials because it had a significantly lower thermal conductivity [13].

2.5 Die-Attach Properties

Conductive adhesives normally cure at temperatures far lower than those needed for soldering, which can exceed 250°C. Temperatures between 80°C and 180°C are often used while conducting adhesive cure, depending on the adhesive type and application. They can be used to attach temperature-sensitive components, like flexible electronics and semiconductors, which could be harmed by greater soldering temperatures, because of their lower curing temperature. Certain epoxy conductive adhesives containing silver, for example, have a curing temperature range of 120°C to 150°C, while adhesives made for expedited processing have a slightly higher curing temperature. Moreover, these adhesives are significantly more flexible than solder, making them more suitable for withstanding substrate bending. Lead- and solvent-free conductive adhesives provide an additional benefit over soldering [26].

The performance of the device during operation is further affected by die-attach, which provides thermal or electrical conductivity between the die and the packaging as mentioned by Yarmand *et al.,*[20]. Table 2 displays additional material attributes and results that were used as a baseline input for FEA modelling in order to calculate the overall heat flux. The die-attach domain was divided into 8 samples with progressively increased thermal conductivity, starting at 0 W/mK which is specifically 0.698 W/mK, and increasing to 350 W/mK, with each sample interval representing 50 W/mK without affecting the density and specific heat data. Galson *et al.,* [30] stated that thermal conductivity measurements are crucial for evaluating terrestrial heat flow, with various methods available. The divided-bar and Quick Thermal Conductivity Meter (QTM) techniques have been compared, revealing that QTM requires at least 5-6 measurements per sample for isotropic rocks and twice as many for anisotropic rocks. Based on experimental findings or material properties from past research on graphene-based composites, the thermal conductivity of 0.698 W/m.K. is selected in some studies [13,20]. This number may represent the lower end of thermal conductivity for composite materials, for instance, in configurations where defects, filler concentration, and matrix dispersion affect thermal performance [29].

In thermal analysis, there are numerous significant advantages to beginning with a low thermal conductivity value, such as 0.698 W/m·K. A more accurate evaluation of the conductive ink's efficacy is made possible by the baseline it creates for evaluating the performance of materials with greater thermal conductivities. Lower results for thermal conductivity may indicate less conductive or optimized forms of the ink, providing information on how less sophisticated formulations function in comparison to more conductive ones. Since inks with variable conductivities are employed in practical applications, it is helpful to start with a lower value to predict how various ink formulations would react to heat stress in realistic situations. Furthermore, this method helps comprehend how sensitive the thermal behaviour of the model is to variations in thermal conductivity, which is an important understanding. Additionally, Nguyen *et al.,* [34], stated that composite inks with low thermal conductivity can be used to directly print thermal management devices like heat sinks. Therefore, in this research were investigated too about how low thermal conductivity affects temperature distribution and heat flux, especially in hybrid materials that include graphene and silver nanoplatelets.

The material parameters from GNP/Ag 1 to GNP/Ag 8, which represented the thermal conductivity of die-attach materials, are displayed in Table 3 and were employed in the FEA simulation analysis.

Table 2
Material properties based on Kamal *et al.,* [13]

Materials	Properties		
	Density (kg/m^3)	Thermal conductivity (W/m.K)	Specific heat (J/kg.K)
SiC (Diode)	3215	120	650
GNP/Ag	997.9	0.698	378.57
Copper	8300	401	385

Table 3
Calculated material resistance and heat flux

Materials	Thermal Conductivity (W/m.K)
GNP/Ag 1	0.698
GNP/Ag 2	50
GNP/Ag 3	100
GNP/Ag 4	150
GNP/Ag 5	200
GNP/Ag 6	250
GNP/Ag 7	300
GNP/Ag 8	350

2.6 Heat Flux

Heat flux and temperature are related in the thermal system. In order to comprehend heat transport processes, temperature is an essential component of all thermal systems. In contrast, heat flux is defined as the energy in transit to a temperature difference per unit cross-sectional area normal to the direction of the flux. Variations in heat flow can cause temperature fluctuations throughout a material, which in turn affects temperature distribution in heat conduction difficulties. Shekar and Krishan [9] elaborate on the heat flux impact of GNP/Ag die-attach adhesives with respect to different types of substrate sizes with increasing thermal conductivity. Cebula *et al.,* [27] use the solution of an Inverse Heat Conduction Problem (IHCP) to find the local heat flux and temperature distribution on a thick cylindrical surface. In order to evaluate thermal conductivity between all die-attach material models, heat flux was applied to the diode surface through to the substrate. On the different die-attach models, the total heat flux can be calculated using Eq. (2). Fourier's law of heat conduction [13,28] can be applied to calculate the heat flux:

$$q = k(dT/dx) \tag{2}$$

The heat flux (W/m^2) is denoted by *q, dT* is the temperature of heat applied to the top surface of the diode with T_1 = 90.3 ^{0}C (measured in Kelvin) to the bottom surface of the substrate (T_2 = 24 ^{0}C), material thickness is represented by *dx*, and the thermal conductivity coefficient (measured in W/m.K) by *k*.

3. Result and Discussion

3.1 Numerical Result

In this work, the relationship between heat flux and material resistance is examined during a one-second heating period at temperatures ranging from 24°C to 90.3°C. The study aims to determine the best-performing GNP/Ag die-attach material in terms of heat conductivity using transient thermal analysis. A modelling strategy, grounded in thermal theories, was developed to evaluate how varying thermal conductivity of the die-attach materials affects substrates of different sizes. Among the materials tested, GNP/Ag 8, with the highest thermal conductivity of 350 W/m·K, exhibited the highest heat flux in the simulation, reaching 6.6 MW/m² for a 4x4 mm substrate. As the temperature increased over time, the heat flux also increased. The simulation started at an ambient temperature of 90.3°C and reached 24°C within one second. The adaptive time-stepping method was applied to all eight models. After one second, noticeable variations in the colour contours on the surface of the circuit model were observed, representing the heat distribution across the die-attach materials. The finite element analysis (FEA) results for temperature distribution in a 4x4mm substrate for all eight models are shown in Figure 6. Each model's temperature flow is illustrated by distinct contour colours, reflecting their respective thermal conductivities: GNP/Ag 1 (0.698 W/m·K), GNP/Ag 2 (50 W/m·K), GNP/Ag 3 (100 W/m·K), GNP/Ag 4 (150 W/m·K), GNP/Ag 5 (200 W/m·K), GNP/Ag 6 (250 W/m·K), GNP/Ag 7 (300 W/m·K), and GNP/Ag 8 (350 W/m·K).

There is an observation that has been explored which is contour colour variation and heat flow in low vs. high thermal conductivity materials as in Figure 6. For the contour colour variation and heat flow in low vs. high thermal conductivity materials, the limited range of contour colours in low thermal conductivity materials is due to their slower rate of heat transmission. In materials like GNP/Ag 1 (0.698 W/m·K), heat transport is restricted, resulting in a narrow temperature differential across the material. This causes a small portion of the material to undergo significant temperature changes, while most of the material remains close to the initial temperature. Consequently, the contour plot shows fewer colours, indicating low heat distribution. In contrast, materials with higher thermal conductivity, such as GNP/Ag 8 (350 W/m·K), allow heat to flow more uniformly, creating a complex temperature gradient. This results in a contour plot with a wider range of colours. Thus, the simpler colour distribution in low thermal conductivity models reflects limited heat transfer and reduced temperature variation across the substrate.

Meanwhile, the temperature flow and heat flux distribution across different models in Figure 6 illustrates the temperature flow in the models from three perspectives: (a) side view, (b) front view, and (c) back view, along with their corresponding contour colour ranges. The temperature ranges from 90.3°C at the diode surface to 24°C at the lower part of the substrate. Most of the contour plots display a transition from red to blue, indicating the decreasing temperature as heat dissipates toward ambient conditions. The most significant temperature changes occur near the diode, while normal ambient temperatures are observed at the die-attach and substrate due to their thin material layers. However, in GNP/Ag 1 (0.698 W/m·K), the temperature drops drastically from 90.3°C to 75.567°C, and then to 31.367°C. This indicates that in low thermal conductivity materials, where values approach 0 W/m·K, the temperature transition is more exciting, resulting in a blue contour on the substrate surface.

Temperature GNP/Ag 1 - 0.698 W/m.K

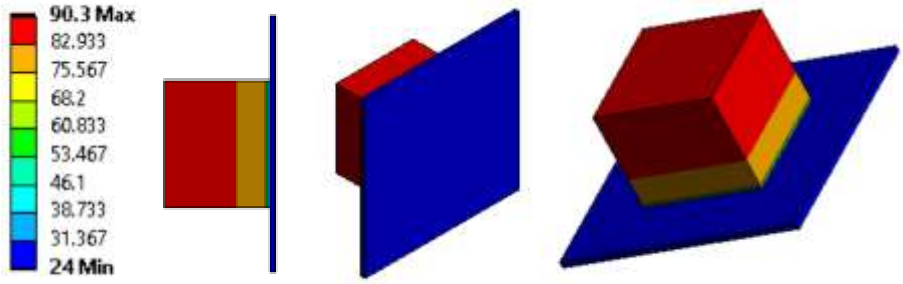

(a) (b) (c)

Temperature GNP/Ag 2 - 50 W/m.K

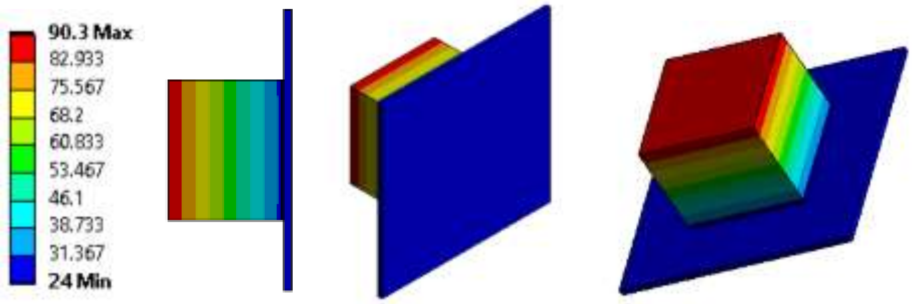

(a) (b) (c)

Temperature GNP/Ag 3 - 100 W/m.K

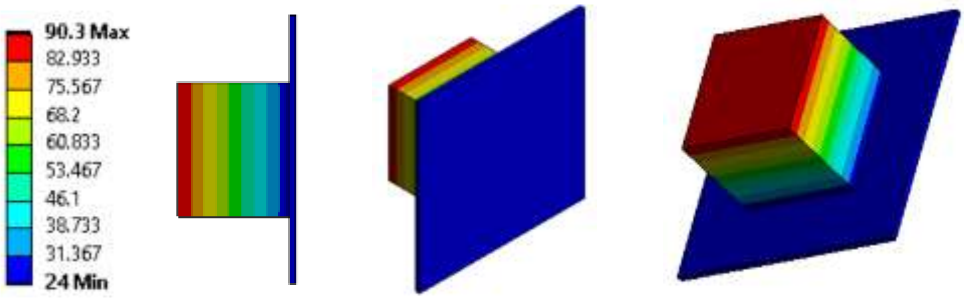

(a) (b) (c)

Temperature GNP/Ag 4 - 150 W/m.K

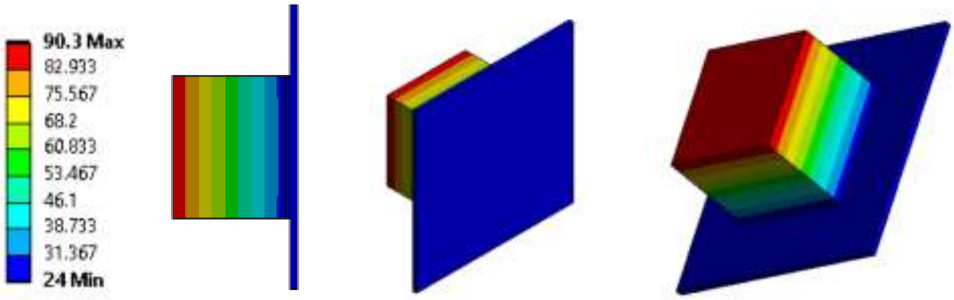

(a) (b) (c)

Temperature GNP/Ag 5 - 200 W/m.K

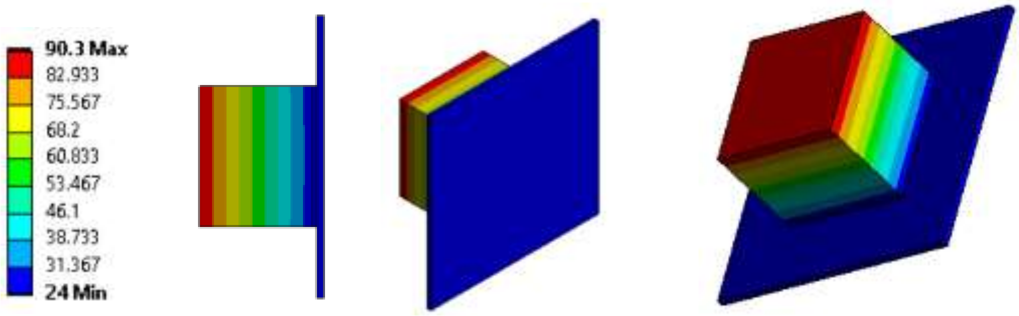

(a) (b) (c)

Temperature GNP/Ag 6 - 250 W/m.K

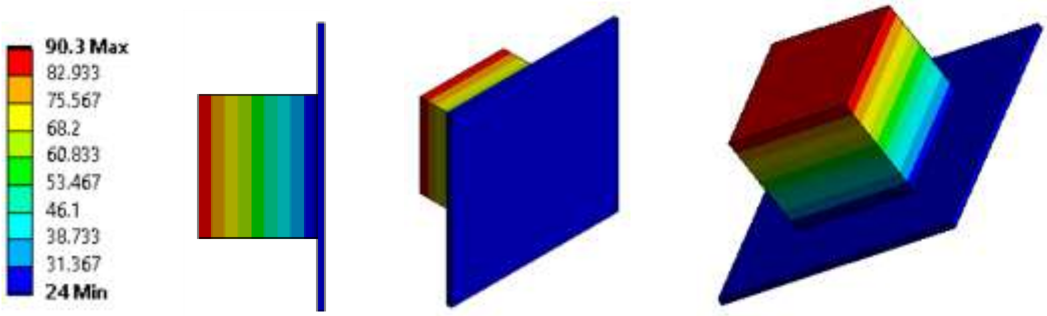

(a) (b) (c)

Temperature GNP/Ag 7 - 300 W/m.K

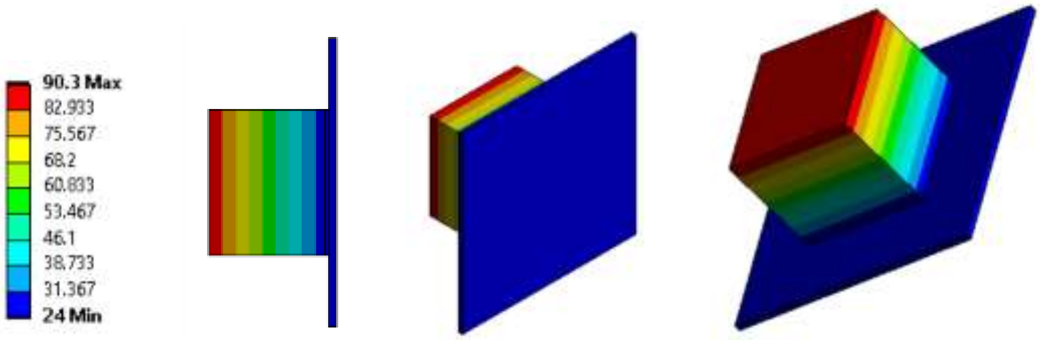

(a) (b) (c)

Temperature GNP/Ag 8 - 350 W/m.K

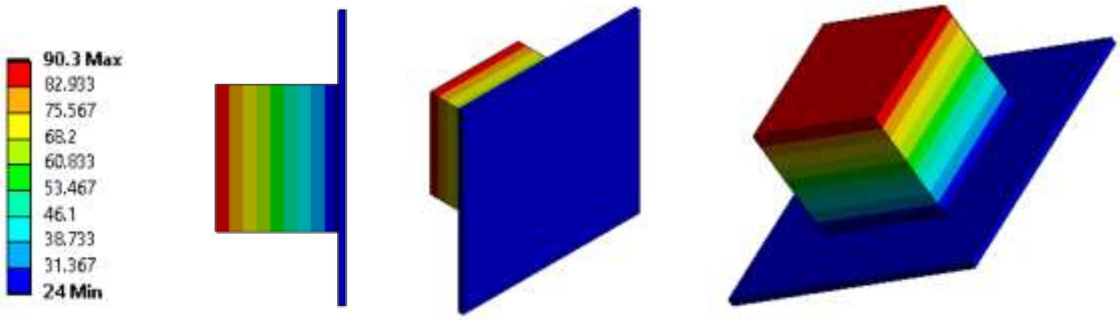

(a) (b) (c)

Fig. 6. Temperature flow for 4mm x 4mm substrate size with all 8 model values of thermal conductivity

In the meantime, Figure 7 shows the total heat flux distribution across the models. In GNP/Ag 1 (0.698 W/m·K), the total heat flux remains at the highest value of 6.986x10^5 W/m². This high heat flux is observed across the diode, die-attach, and substrate materials. In GNP/Ag 2 (50 W/m·K), the total heat flux decreases, starting from 4.992x10^6 W/m. The material's intermediate thermal conductivity accounts for the significant increase in green regions on the substrate surface and the observed decrease in overall heat flow in GNP/Ag 2 (50 W/m·K). GNP/Ag 2, is less efficient than higher conductivity materials like GNP/Ag 8, but it still permits greater heat transfer than lower conductivity materials like GNP/Ag 1. Because the heat is dispersed more evenly throughout the substrate as opposed to being focused in particular areas, as seen in lesser conductivity models, this leads to a lower heat flux value. In the contour plot, regions with a moderate heat flux are indicated by the presence of green areas. This dispersion occurs as a result of the mild conductive nature of GNP/Ag 2, which more evenly distributes the heat across the substrate. High-conductivity materials exhibit a more diversified heat dispersion, whereas low-conductivity materials tend to have heat that stays localized, resulting in fewer colours on the contour plot. Between low and high conductivity materials, GNP/Ag 2 represents a transition region where heat flux is less strong but more uniformly distributed. As a result, the change in heat transfer is more gradual, as seen by the growth of green regions when heat transfers from the die-attach material to the substrate.

For GNP/Ag 3 (100 W/m·K), the heat flux rises again to 5.40 x10^6 W/m², with the diode showing an orange colour, and the die-attach region reaching the highest heat flux in red. The connected materials show significant colour changes, but the substrate surface remains blue, indicating the lowest heat flux values. The greater thermal conductivity of GNP/Ag 3 (100 W/m·K) results in a 5.40 x10^6 W/m² increase in heat flow when compared to GNP/Ag 2. The enhanced thermal conductivity of GNP/Ag 3 (100 W/m·K) facilitates more effective heat transfer. A higher heat flux is the outcome of this enhanced heat conduction, particularly in the die-attach and diode regions. The die-attach zone achieves the maximum heat flux, shown by red in the contour plot, whereas the diode exhibits an orange tint, suggesting an intermediate heat flux. Nevertheless, the substrate surface stays blue, suggesting low heat flow values, even with the increasing heat flux in the die-attach and diode regions. The reason for this is that heat is concentrated around the source (die and die-attach) before it disperses entirely into the substrate because the substrate material has a lesser capacity to conduct heat than the diode and die-attach regions.

The bottleneck caused by the substrate's reduced thermal conductivity, which keeps the heat from spreading as widely, the substrate stays colder and displays lower heat flow values, as indicated by the blue colour. In conclusion, the greater thermal conductivity of GNP/Ag 3 enhances heat transmission in the die-attach and diode regions, while the substrate's reduced capacity to transmit heat restricts the amount of heat flux that reaches the substrate surface, resulting in the observed colour differences. This pattern, seen in the GNP/Ag 4 (150 W/m·K), GNP/Ag 5 (200 W/m·K), and GNP/Ag 6 (250 W/m·K) models, persists because the die-attach material's capacity to transport heat efficiently rises with its thermal conductivity. The substrate surface, on the other hand, continues to be blue, suggesting low heat flux values, even if the connected materials (die-attach and diode) exhibit a noticeable rise in heat flux, represented by the colour changes towards red and green. This occurs because heat cannot completely disperse across the substrate due to the substrate's limited capacity to transfer heat, despite the increased thermal conductivity of the die-attach materials. The substrate stays blue, indicating the ongoing heat flow bottleneck at the substrate level, while the linked materials show more uniform heat transfer, shown by the green colour, when the thermal conductivity approaches GNP/Ag 7 (300 W/m·K). The substrate continues to conduct heat at a different rate than the material, which results in reduced heat flux in the die-attach and diode regions even if the material is now conducting heat efficiently there. The red region, which indicates an intensive heat flux, almost completely vanishes in GNP/Ag 8 (350 W/m·K), the material with the maximum thermal conductivity, as the heat flux becomes more efficiently dispersed among the linked components. The effective heat transmission of this material is demonstrated by the rise in total heat flux to 6.59 x10^6 W/m². The substrate's restrictions keep it from experiencing the same high flux seen in the connected materials, as evidenced by the substrate surface's continued blue coloration despite the increased total heat flow.

Total Heat Flux GNP/Ag 1 - 0.698 W/m.K

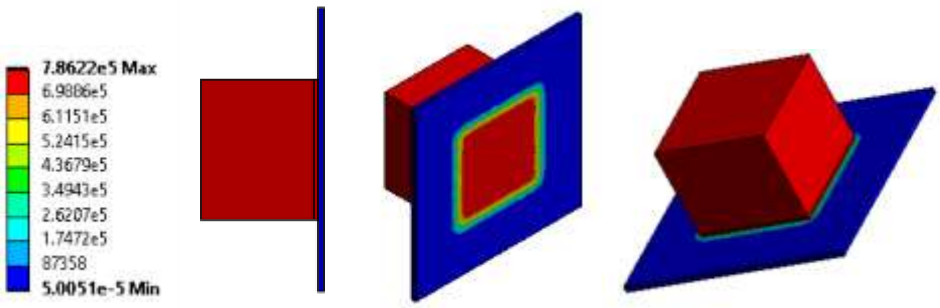

(a) (b) (c)

Total Heat Flux GNP/Ag 2 - 50 W/m.K

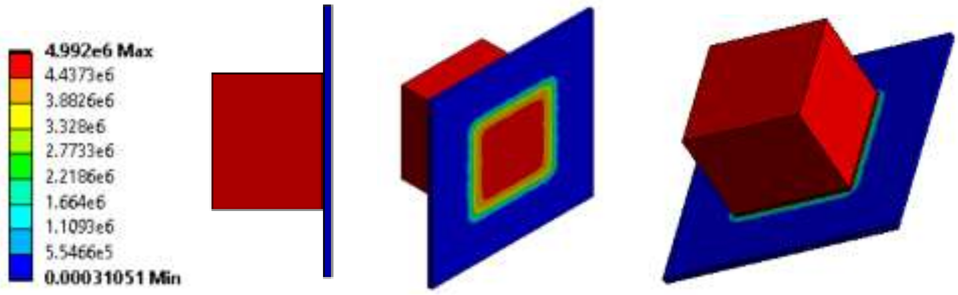

(a) (b) (c)

Total Heat Flux GNP/Ag 3 - 100 W/m.K

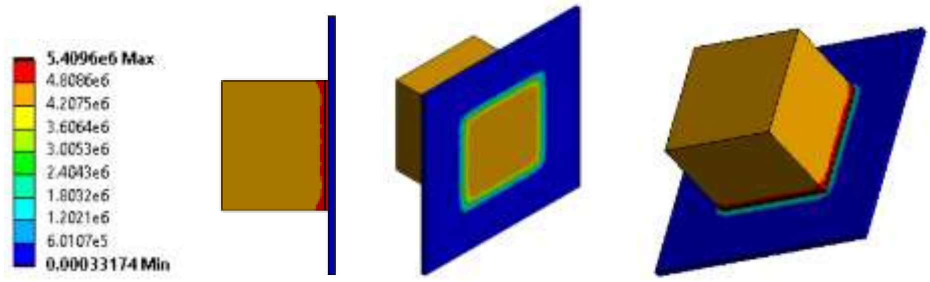

(a) (b) (c)

Total Heat Flux GNP/Ag 4 - 150 W/m.K

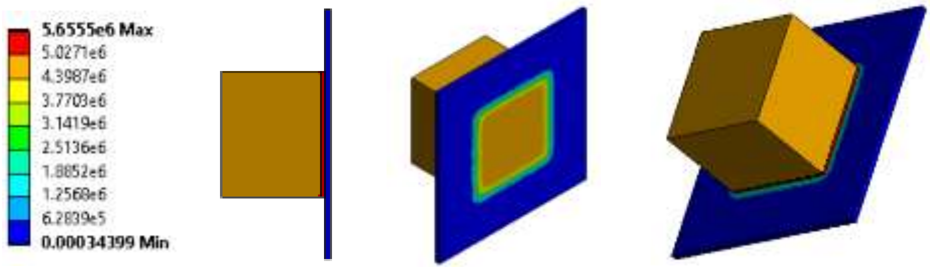

(a) (b) (c)

Total Heat Flux GNP/Ag 5 - 200 W/m.K

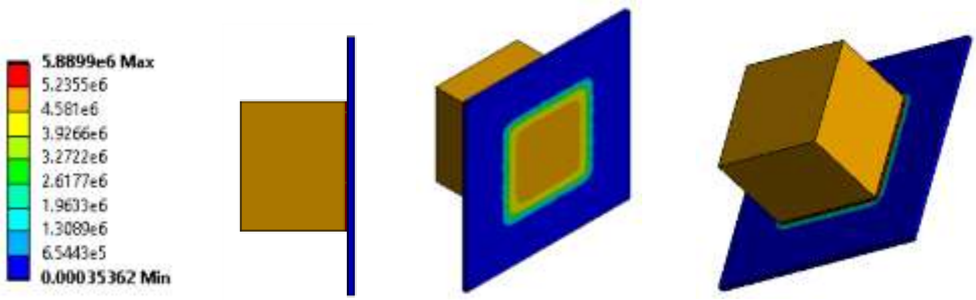

(a) (b) (c)

Total Heat Flux GNP/Ag 6 - 250 W/m.K

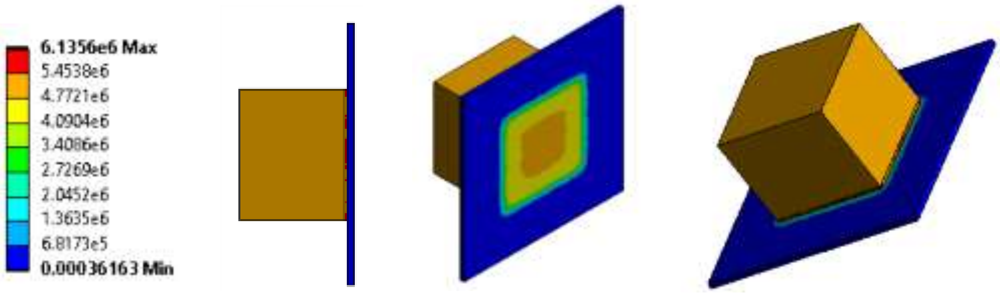

(a) (b) (c)

Total Heat Flux GNP/Ag 7 - 300 W/m.K

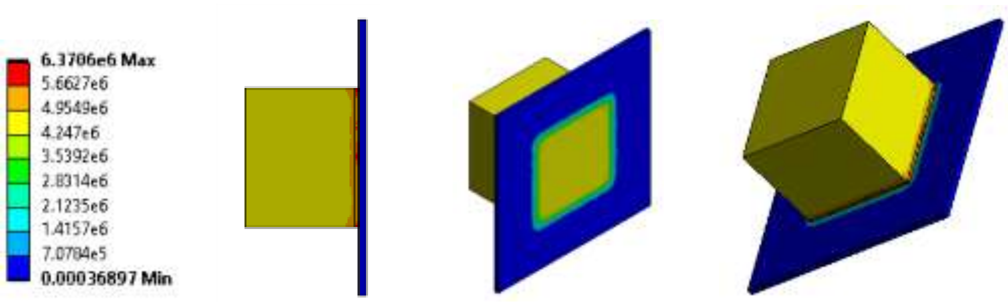

(a) (b) (c)

Total Heat Flux GNP/Ag 8 - 350 W/m.K

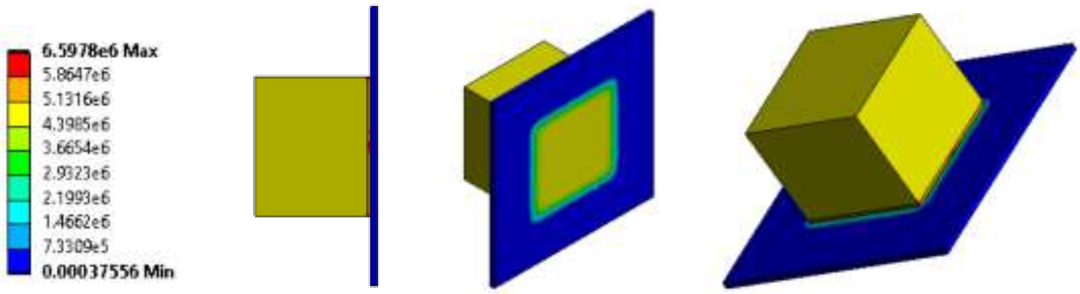

(a) (b) (c)

Fig. 7. Total heat flux flow for 4mm x 4mm substrate size with all 8 model values of thermal conductivity

This demonstrates that the most total heat flow is seen on 4x4 mm substrates since the GNP/Ag 8 model's enhanced thermal conductivity permits the best possible heat transfer in the die-attach and diode regions. Nevertheless, the amount of heat distribution throughout the system is constrained by the substrate's very low thermal conductivity. In the GNP/Ag 8 model with improved thermal conductivity, in particular, the phenomena where the maximum overall heat flow is observed on 4x4 mm substrates can be explained by the material's effective heat transfer in the die-attach and diode regions. The thermal conductivity of GNP/Ag 8 is 350 W/m·K, which guarantees optimal heat conduction and prompt and efficient transfer of the heat generated in the diode through the die-attach layer. In these areas, heat is transmitted with little resistance, resulting in high heat flow values. A bottleneck is created when the heat cannot pass through and into the substrate due to the decreased conductivity. Heat cannot spread uniformly throughout the system because of the substrate's uneven heat-conduction rate, despite the die-attach and diode areas' efficient heat-transfer capabilities. Therefore, even though there is significant heat transfer seen in the die-attach and diode regions, the substrate's reduced thermal conductivity limits the overall amount of heat distribution. The 4x4 mm substrate size maximizes overall heat flow because it enables the system to strike an ideal compromise between the substrate's constraints and the diode/die-attach's heat transfer efficiency. The heat is concentrated because the substrate's reduced size further restricts heat dissipation.

3.3 Relationship between Heat Flux and Substrate Size

Figure 8 shows the total heat flow values for the GNP/Ag die-attach materials, as determined by transient thermal analysis at the maximum thermal conductivity of 350 W/m.K. across a range of substrate sizes (in millimeters). The colour contour of the model is strongly influenced by the heat produced on the substrate surface. In Figure 8(a), the model displays little changes and the heat flux has little effect on a 2x2mm substrate. The majority of the contour in blue indicates low heat flux values. This implies that the heat flux from the die-attach material is not efficiently captured by the smallest substrate size. As the substrate size rises, however, Figures 8 (b), (c), and (d) demonstrate more noticeable colour variations (4x4 mm, 8x8 mm, and 16x16 mm, respectively). In contrast, larger substrates allow for greater heat distribution.

The transition of contour colours from blue to red in Figures 8 (b), (c), and (d) illustrates this effect. The increased substrate size facilitates more effective heat transfer from the die-attach material, leading to a broader range of colours and higher heat flux values. The most significant effect is observed in Figure 8 (e) with the 32x32mm substrate, where the maximum heat flux is highlighted in red. The larger substrate area accommodates and distributes heat more uniformly, resulting in a colour transition to light brown, particularly around the die-attach and substrate connection area. This indicates that the larger substrate enhances overall heat dissipation, as the heat can reach and effectively spread across the outer surface of the substrate.

The colour contour starts to change from blue to red, signifying a rise in the values of heat flow. The greatest substrate size, 32x32 mm, is the one that has the biggest impact in Figure 8(e), where the maximum heat flow value is indicated in red. When heat flow reaches the substrate's outer surface, the contour changes to a light brown hue, especially in the area of the die-attach and substrate connection areas. This shift implies that heat is dispersed throughout the greater substrate area. Each subfigure has an explanation that explains why the light brown colour is closer to red, which denotes a higher heat flow. The die-attach area, where the largest heat flux is focused, is where this is most noticeable. As thermal conductivity rises, the heat flux rises significantly as well, particularly between 0.698 and 50 W/m.K. After that, when thermal conductivity rises, the heat flux increases more gradually and reaches its maximum at 350 W/m.K. This pattern shows that although thermal conductivity typically increases with heat flux, the largest changes take place around the lower end of the conductivity spectrum, with more moderate gains occurring at higher conductivity levels. In summary, the results demonstrate that larger substrate sizes enable more efficient heat transfer and distribution, leading to more pronounced changes in heat flux and colour contours compared to smaller substrates. This trend underscores the impact of substrate size on heat management and distribution within the system.

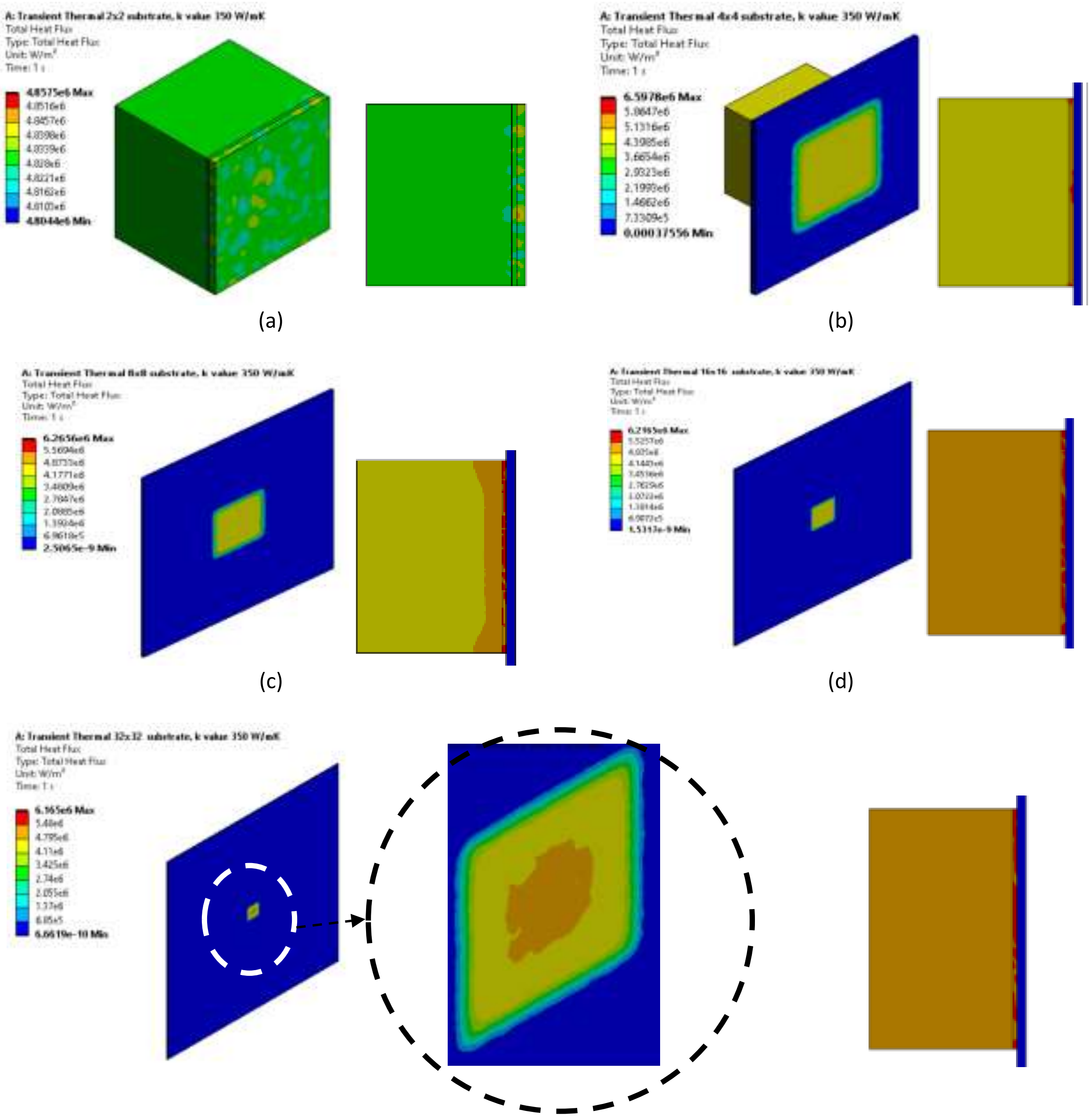

Fig. 8. Total heat flux result of GNP/Ag hybrid die-attach materials using transient thermal analysis in different substrate perimeter saiz at the maximum value of thermal conductivity, 350 W/mK. (a) 2x2 mm (b) 4x4 mm (c) 8x8 mm (d) 16x16 mm and (e) 32x32 mm

Figure 9 shows an interesting trend in the interaction between heat flux, thermal conductivity, and GNP/Ag die-attach materials. When the substrate size approaches 4x4 mm, the heat flux begins to level out even though the overall heat flux value rises and the colour contour shifts across the model. The overall heat flux drops when the substrate size is increased to 8x8 mm; this dip is visible on the graph below the 4x4 mm substrate line. For bigger substrate sizes, such as 16x16 mm and 32x32 mm, this trend is still present. This effect happens as a result of the substrate's larger surface area, which permits more heat dissipation when the size surpasses 4x4 mm. Because of the increased surface area's ability to disperse heat, the total heat flux value at the substrate is lowered. Stated differently, as the surface area increases, the model's ability to control and release heat decreases, which results in a drop in heat flux values above the ideal 4x4 mm substrate size. As a result, the 4x4 mm substrate size is found to be the best choice for managing and containing heat. It maintains an ideal heat flux by striking a balance between effective heat retention and efficient heat transport, hence avoiding excessive dispersion.

In addition, the graph exhibits a steady trend in total heat flow, showing an increase in substrate size from 2x2 mm to 4x4 mm, followed by a nearly constant value at 8x8 mm. Beyond the 4x4 mm substrate size, the heat flux gradually increases for larger substrates, particularly at 16x16mm and 32x32 mm. According to Attinger et al., [22], this finding suggests that the 4x4 mm substrate offers the optimal balance between surface area and thermal conductivity, thus enhancing heat transfer efficiency. Conversely, larger substrates tend to dissipate heat over a broader surface area, which may result in a reduction of overall heat flux.

This behaviour aligns with the pattern observed for the 8x8 mm, 16x16 mm, and 32x32 mm substrates, where the peak heat flux at 4x4 mm is followed by a gradual rise in total heat flux. The relationship between thermal conductivity and substrate size is significant because changes in substrate dimensions can influence heat transfer behaviour. Research has shown that variations in substrate size can affect a material's heat-conducting capacity due to factors such as heat transfer pathways and thermal boundary conditions. Larger substrates tend to interact more with their surroundings, leading to increased heat dissipation and, possibly, greater heat losses.

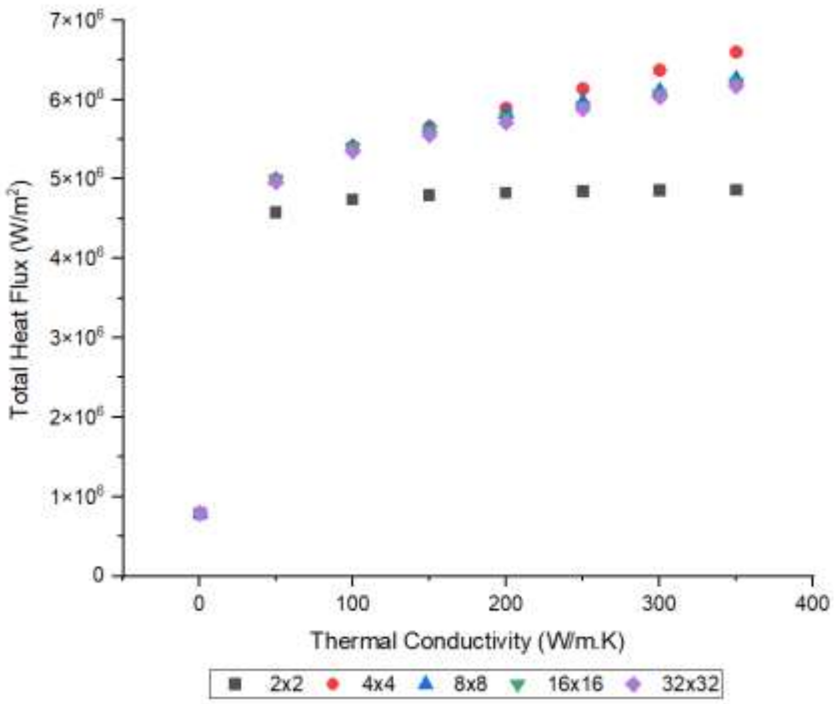

Fig. 9. Heat Flux vs Thermal Conductivity vs GNP/Ag

The relatively small difference in total heat flux between the 4x4 mm and 8x8 mm sizes observed in this study is attributed to the balance between surface heat dissipation and internal heat conduction. As substrate size increases, more heat transfer pathways become available, improving heat conduction. However, the larger surface area also leads to greater heat loss to the environment. This dynamic may explain the slower increase in heat flux between these sizes compared to others. Previous research on thermochemical lithography, thermal conductivity of micro- and nanoparticle composites, and the influence of particle size on heat transfer has shown that greater heat dissipation over a larger area can result in lower effective thermal conductivity for larger substrates or composite materials.

Several factors can be considered to explain the phenomenon where the highest heat flux is observed in the 4x4mm substrate, followed by a decrease as the substrate size increases (8x8 mm, 16x16 mm, and 32x32 mm):

i) Surface Area to Volume Ratio: Smaller substrates, such as the 4x4 mm size, have a higher surface area to volume ratio. This leads to a more concentrated and intense heat flux, as the heat generated within the material travels a shorter distance to the surface. As substrate size increases, the surface area to volume ratio decreases, causing the heat flux to disperse over a wider region and lose concentration, thereby reducing the overall value [31].
ii) Thermal Gradient: Smaller substrates exhibit a steeper thermal gradient (temperature difference over a distance) since heat does not need to travel as far. The sharp thermal gradient results in higher heat flux. As substrate size increases, heat dissipation improves, which lowers the localized heat flux [31].
iii) Heat Dissipation: The thermal conductivity of the substrate material plays a critical role in heat transfer. Materials with higher thermal conductivity enhance heat dissipation [32]. Larger substrates can absorb and release more heat, dispersing it over a greater volume, thus reducing the total heat flux at any given point. In contrast, smaller substrates reach higher temperatures more quickly and exhibit higher localized heat flux values due to the limited amount of material available to absorb heat.
iv) Boundary Effects: In smaller substrates, boundary effects are more pronounced, directly influencing heat conduction. These substrates exhibit higher heat flux due to steeper thermal gradients and stronger boundary effects [33]. Larger substrates, with more room for heat to disperse, may exhibit concentrated heat flux near the edges.

When these factors are combined, the 4x4 mm substrate demonstrates a higher overall heat flux than larger substrates. This is a common result when performing thermal analysis on materials of varying sizes.

The interaction between GNP/Ag in conductive ink is very important for enhancing both thermal conductivity and stability, particularly when modeled through FEA to simulate heat transfer and electrical performance in various applications. The GNP, renowned for their exceptional thermal and electrical conductivity, form the foundational component of the ink. When incorporated into the ink, GNPs provide a high surface area and excellent electron mobility, enabling efficient thermal dissipation. The direct interaction between GNP and Ag particles enhances the formation of conductive networks, leading to an efficient thermal pathway through the ink. The high aspect ratio of GNP allows for effective load distribution, ensuring that the heat is rapidly spread across the material rather than concentrated at localized points, which could lead to thermal hotspots. In FEA models, this is represented by a reduction in thermal resistance and a more even heat distribution.

The Ag, because the larger particle size and high conductivity, contribute significantly to the stability and overall conductive properties of the ink. These Ag provide macroscopic conductive pathways, creating a robust, continuous conductive matrix that complements the nanostructured network formed by GNPs. In FEA simulations, the Ag help ensure electrical stability by reducing percolation thresholds and enhancing the overall conductivity of the ink. They also serve to minimize the degradation of the ink's properties over time by preventing oxidation, especially in high-temperature environments.

Meanwhile, the SA, which decomposes upon thermal curing, converts into metallic Ag, further enhancing the conductivity of the ink. The Ag network formed through this process acts synergistically with the GNP and Ag to create a dense, interconnected network that significantly improves both thermal and electrical performance. In finite element models, the thermal conductivity is augmented by the enhanced network formation, providing more efficient heat conduction.

Together, the interactions of GNP, Ag, and SA lead to a conductive ink that demonstrates improved thermal dissipation, stability, and long-term reliability, where it is the important factors for advanced electronic and thermal management applications.

4. Conclusion

The study successfully demonstrated the optimal heat conductivity performance of GNP/Ag die-attach materials with varying thermal conductivities using transient thermal analysis. A modeling approach grounded in thermal theories was developed to assess the effects of different thermal conductivity die-attach materials on semiconductor devices and substrate materials. Among the tested substrate sizes, GNP/Ag 8, with the highest thermal conductivity of 350 W/m.K, yielded the highest heat flux value of 6.6 MW/m^2, particularly at the 4x4 mm substrate size. This result highlights the superior performance of the 4x4 mm substrate, especially when used with a diode and die-attach size of 2x2 mm.

The conductive ink offers multiple benefits across various industries due to its broad application potential. Graphene-based conductive ink is cost-effective to manufacture, requiring only a simple process to produce the ink, which can be dried at low temperatures. Moreover, it is environmentally friendly, maintenance-free, and highly durable. Its flexibility and stretchability make it capable of passing bending tests, thus enhancing its dynamic performance. In conclusion, the study's findings on substrate size materials' effects on graphene-based conductive ink will contribute to advancing current technologies. The performance of this conductive ink will continue to surpass that of materials less frequently used in similar applications.

Acknowledgement

This research was not funded by a grant from Ministry of Higher Education of Malaysia. Thanks to Advanced Academia-Industry Collaboration Laboratory (AiCL) and Fakulti Teknologi dan Kejuruteraan Mekanikal (FTKM), Universiti Teknikal Malaysia Melaka (UTeM) for providing the laboratory facilities.

References

[1] He, Pei, Jianyun Cao, Hui Ding, Chongguang Liu, Joseph Neilson, Zheling Li, Ian A. Kinloch, and Brian Derby. "Screen-printing of a highly conductive graphene ink for flexible printed electronics." *ACS applied materials & interfaces* 11, no. 35 (2019): 32225-32234. https://doi.org/10.1021/acsami.9b04589

[2] Camargo, Jessica Rocha, Luiz Otavio Orzari, Diele Aparecida Gouveia Araujo, Paulo Roberto de Oliveira, Cristiane Kalinke, Diego Pessoa Rocha, Andre Luiz dos Santos et al. "Development of conductive inks for electrochemical sensors and biosensors." *Microchemical Journal* 164 (2021): 105998. https://doi.org/10.1016/j.microc.2021.105998

[3] Pillai, Adarsh Sivan, Achu Chandran, and Surendran Kuzhichalil Peethambharan. "MWCNT Ink with PEDOT: PSS as a multifunctional additive for energy efficient flexible heating applications." *Applied Materials Today* 23 (2021): 100987. https://doi.org/10.1016/j.apmt.2021.100987

[4] Huang, Qijin, and Yong Zhu. "Printing conductive nanomaterials for flexible and stretchable electronics: A review of materials, processes, and applications." *Advanced Materials Technologies* 4, no. 5 (2019): 1800546. https://doi.org/10.1002/admt.201800546

[5] Yadav, Vivek Kumar. "Bn doping in the realm of two-dimensional fullerene network for unparalleled structural, electronic, optical, and her advancements: A cutting-edge dft investigation." *arXiv preprint arXiv:2308.06723* (2023).

[6] Bessaguet, Camille, Eric Dantras, Guilhem Michon, Mathieu Chevalier, Lydia Laffont, and Colette Lacabanne. "Electrical behavior of a graphene/PEKK and carbon black/PEKK nanocomposites in the vicinity of the percolation threshold." *Journal of Non-Crystalline Solids* 512 (2019): 1-6. https://doi.org/10.1016/j.jnoncrysol.2019.02.017

[7] Yarmand, Hooman, Samira Gharehkhani, Goodarz Ahmadi, Seyed Farid Seyed Shirazi, Saeid Baradaran, Elham Montazer, Mohd Nashrul Mohd Zubir, Maryam Sadat Alehashem, S. N. Kazi, and Mahidzal Dahari. "Graphene nanoplatelets–silver hybrid nanofluids for enhanced heat transfer." *Energy conversion and management* 100 (2015): 419-428. https://doi.org/10.1016/j.enconman.2015.05.023

[8] Khanafer, Khalil, Kambiz Vafai, and Marilyn Lightstone. "Buoyancy-driven heat transfer enhancement in a two-dimensional enclosure utilizing nanofluids." *International journal of heat and mass transfer* 46, no. 19 (2003): 3639-3653. https://doi.org/10.1016/S0017-9310(03)00156-X

[9] Shekar, Balla Chandra, and Naikoti Kishan. "Finite element analysis of natural convective heat transfer in a porous square cavity filled with nanofluids in the presence of thermal radiation." In *Journal of Physics: Conference Series*, vol. 662, no. 1, p. 012017. IOP Publishing, 2015. https://doi.org/10.1088/1742-6596/662/1/012017

[10] Sudhindra, Sriharsha, Lokesh Ramesh, and Alexander A. Balandin. "Graphene thermal interface materials–state-of-the-art and application prospects." *IEEE Open Journal of Nanotechnology* 3 (2022): 169-181. https://doi.org/10.1109/OJNANO.2022.3223016

[11] Azli, Daniel Azlan Mohd, Mohamad Shukri Zakaria, Mizah Ramli, Ghazali Omar, Mohd Nur, Azmi Nordin, Syahin Syaifuddin, Andee Faeldza Dziaudin, and Abdullah Halim Lim Abdullah. "Equivalent Plastic-Strain Analysis of Copper Stretchable Electronic Circuit Using Finite Element Analysis." *Journal of Advanced Research in Applied Sciences and Engineering Technology* 30, no. 1, (2023):31–43. https://doi.org/10.37934/araset.30.1.3143

[12] Wahid, Ameeruz Kamal Ab, Mohd Azli Salim, Nor Azmmi Masripan, Chonlatee Photong, Adzni Md Saad, and Mohd Zaid Akop. "Transient Thermal Simulation Analysis of Die-Attach Adhesives." *International Journal of Nanoelectronics & Materials* 15 (2022).

[13] Wahid, Ameeruz Kamal Ab, Mohd Azli Salim, Nor Azmmi Masripan, Chonlatee Photong, Adzni Md Saad, Mohd Zaid Akop, and Muhd Ridzuan Mansor. "Numerical Analysis of GNP/Ag Die-Attach Adhesives with Different Thermal Conductivity." *International Journal of Nanoelectronics & Materials* 15 (2022).

[14] Zhang, Tao. "Ansys second development method and application in transient thermal simulation." In *2008 International Conference on Computer Science and Software Engineering*, vol. 2, pp. 643-645. IEEE, 2008. https://doi.org/10.1109/CSSE.2008.1078

[15] Cremonesi, Massimiliano, Alessandro Franci, Sergio Idelsohn, and Eugenio Oñate. "A state of the art review of the particle finite element method (PFEM)." *Archives of Computational Methods in Engineering* 27, no. 5 (2020): 1709-1735. https://doi.org/10.1007/s11831-020-09468-4

[16] Yang, Jun. "Finite Element Simulation of Graphene Thermal Conductivity Framework." In *MATEC Web of Conferences*, vol. 358, p. 01065. EDP Sciences, 2022. https://doi.org/10.1051/matecconf/202235801065

[17] Arif, Muhammad Shoaib, Kamaleldin Abodayeh, and Yasir Nawaz. "An Application of the Finite Element Method for Heat and Mass Transfer of Boundary Layer Flow Using Variable Thermal Conductivity and Mass Diffusivity." *Journal of Mathematics* 2022, no. 1 (2022): 7929161. https://doi.org/10.1155/2022/7929161

[18] Akeremale, Collins O., Olusegun A. Olaiju, and Yeak Su Hoe. "Finite Element Method for Heat Transfer Phenomenon on a Closed Rectangular Plate." *EUREKA: Physics and Engineering* 5 (2020): 91. https://doi.org/10.21303/2461-4262.2020.001422

[19] Childs, P. R. N., J. R. Greenwood, and C. A. Long. "Heat flux measurement techniques." *Proceedings of the Institution of Mechanical Engineers, Part C: Journal of Mechanical Engineering Science* 213, no. 7 (1999): 655-677. https://doi.org/10.1177/095440629921300702

[20] Yarmand, Hooman, Samira Gharehkhani, Goodarz Ahmadi, Seyed Farid Seyed Shirazi, Saeid Baradaran, Elham Montazer, Mohd Nashrul Mohd Zubir, Maryam Sadat Alehashem, S. N. Kazi, and Mahidzal Dahari. "Graphene nanoplatelets–silver hybrid nanofluids for enhanced heat transfer." *Energy conversion and management* 100 (2015): 419-428. https://doi.org/10.1016/j.enconman.2015.05.023

[21] Okereke, Michael, and Simeon Keates. "Finite element applications." *A Practical Guide to the FEMA Process. TextBook. Publisher: Springer* (2018). https://doi.org/10.1007/978-3-319-67125-3

[22] Kamyshny, Alexander, and Shlomo Magdassi. "Conductive nanomaterials for 2D and 3D printed flexible electronics." *Chemical Society Reviews* 48, no. 6 (2019): 1712-1740. https://doi.org/10.1039/C8CS00738A

[23] Shekar, Balla Chandra, and Naikoti Kishan. "Finite element analysis of natural convective heat transfer in a porous square cavity filled with nanofluids in the presence of thermal radiation." In *Journal of Physics: Conference Series*, vol. 662, no. 1, p. 012017. IOP Publishing, 2015. https://doi.org/10.1088/1742-6596/662/1/012017

[24] Ovrebo, Gregory K. *Thermal simulation of four die-attach materials*. Army Research Laboratory, 2008. https://doi.org/10.21236/ADA477276

[25] Qiang, Jun, and Tao Peng. "Optimization of Substrate Sizes for In Situ Stress Measurement in Electrodeposits Relying on Nonlinear Effects." *Coatings* 13, no. 12 (2023): 2031. https://doi.org/10.3390/coatings13122031
[26] Rizwee, Mumtaz, and Deepak Kumar. "Evaluating residual stresses in metal additive manufacturing: a comprehensive review of detection methods, impact, and mitigation strategies." *International Journal of Material Forming* 17, no. 6 (2024): 53. https://doi.org/10.1007/s12289-024-01855-7
[27] Cebula, Artur, Jan Taler, and Pawel Ocłoń. "Heat flux and temperature determination in a cylindrical element with the use of Finite Volume Finite Element Method." *International journal of thermal sciences* 127 (2018): 142-157. https://doi.org/10.1016/j.ijthermalsci.2018.01.022
[28] Lienhard, John H. *A heat transfer textbook*. Phlogistron, 2005.
[29] Zhao, Meng, Wei Pan, Chunlei Wan, Zhixue Qu, Zheng Li, and Jun Yang. "Defect engineering in development of low thermal conductivity materials: A review." *Journal of the European Ceramic Society* 37, no. 1 (2017): 1-13. https://doi.org/10.1016/j.jeurceramsoc.2016.07.036
[30] Galson, D. A., N. P. Wilson, U. Schärli, and L. Rybach. "A comparison of the divided-bar and QTM methods of measuring thermal conductivity." *Geothermics* 16, no. 3 (1987): 215-226. https://doi.org/10.1016/0375-6505(87)90001-0
[31] Lu, T. J., A. G. Evans, and J. W. Hutchinson. "The effects of material properties on heat dissipation in high power electronics." (1998): 280-289. https://doi.org/10.1115/1.2792634
[32] Durgam, Shankar, Ajinkya Bhosale, Vivek Bhosale, Revati Deshpande, and Pankaj Sutar. "Thermal aspect of material selection for substrate board equipped with high heat flux IC chips." In *IOP Conference Series: Materials Science and Engineering*, vol. 1091, no. 1, p. 012005. IOP Publishing, 2021. https://doi.org/10.1088/1757-899X/1091/1/012005
[33] Krishnamoorthy, Shriram, and Masud H. Chowdhury. "Analysis of Spatial Temperature Distribution in ICs." In *2007 14th IEEE International Conference on Electronics, Circuits and Systems*, pp. 1272-1275. IEEE, 2007. https://doi.org/10.1109/ICECS.2007.4511229
[34] Nguyen, Nam, Eric Melamed, Jin Gyu Park, Songlin Zhang, Ayou Hao, and Richard Liang. "Direct printing of thermal management device using low-cost composite ink." *Macromolecular Materials and Engineering* 302, no. 10 (2017): 1700135. https://doi.org/10.1002/mame.201700135